Eigenmodal resonances of polydisperse bubble systems on a rigid boundary

Suhith Illesinghe and Andrew Ooi[a)]
Department of Mechanical Engineering, The University of Melbourne, Parkville, Victoria 3010, Australia

Richard Manasseh
Fluid Dynamics Group, CSIRO Materials Science and Engineering, Highett, Victoria 3190, Australia

(Received 5 March 2009; revised 15 July 2009; accepted 5 October 2009)

This paper presents theory and experimental data on the resonance frequency of systems consisting of different-sized air bubbles attached to a rigid wall. Effects of the change in resonant frequency with bubble size and distance between the bubbles were studied. It was found that the symmetric mode resonance frequency of the bubble system decreased with increasing $r=R_{02}/R_{01}$, where R_{01} and R_{02} are the equilibrium radii of bubbles in the system. Both the symmetric and antisymmetric modes of oscillation were detected in the experiments, with the resonant frequency of the symmetric mode dominant at small bubble separation and the frequency of the antisymmetric mode dominant when the bubbles were farther apart. A linear coupled-oscillator theoretical model was used to describe the oscillations of the bubble system, in which the method of images was used to approximate the effects of the wall. It was found that there was fair to good agreement between the predictions of the coupled-oscillator model with the experimental data.
 [DOI: 10.1121/1.3257581]

PACS number(s): 43.35.Bf, 43.20.Fn, 43.20.Px, 43.20.Bi [RR] Pages: 2929–2938

I. INTRODUCTION

The expansion and compression of gas bubbles within a liquid medium was first studied theoretically by Lord Rayleigh[1] in 1917. The mathematical model originally considered by Rayleigh has been modified over the years by many researchers.[2–4] One such model is the nonlinear Rayleigh–Plesset equation which like Rayleigh's original derivation assumes that the bubbles remain spherical. It has been well-known that the nonlinear dynamics of the Rayleigh–Plesset equation is only relevant for small (micron sized) bubbles. Large (millimeter sized) bubbles typically undergo very small oscillations, thus experiencing simpler dynamics governed by a linear second order ordinary differential equations, derived by linearizing the Rayleigh–Plesset equation. The natural frequency of this linearized model is commonly used to estimate the resonant frequency of an isolated bubble oscillating in response to acoustic excitation. This frequency, commonly known as the Minnaert's frequency, was also independently derived by Minnaert.[5]

The early studies mentioned above only considered cases where the bubbles were assumed to exist in isolation. More recently, systems consisting of many interacting bubbles have been studied by various investigators.[6–15] A short review of some recent studies can be found in the article by Manasseh and Ooi.[16] As one might expect, bubbles can interact acoustically with each other, causing the natural frequencies of the system to change from that of isolated bubbles, and it was found that the interaction has a greater effect when the bubbles are closer. (These modifications to the system frequencies are linear effects; it had been known for some time that nonlinearities can cause interacting bubbles to move, a phenomenon called the secondary Bjerknes effect, e.g., Ref. 17.) In order to model the linear interaction, Feuillade[8] used the coupled oscillator approach by modeling the system as a coupled set of ordinary differential equations, using the self-consistent formulation introduced by Tolstoy[7] and showed that the predicted data agree well with available experimental data. In the same article, Feuillade conducted mathematical analyses of two and three bubble systems and showed that there are various natural oscillating modes of the bubbles such as symmetric, or "+," (where all bubbles oscillate in phase) and antisymmetric, or "−," (where all bubbles oscillate 180° out of phase) modes. If the bubble system oscillates in the − mode, a phenomena known as super-resonances can occur. In this state, the overall damping of the bubble system is small and the bubbles can undergo very large oscillations (see Ref. 18 for more detailed explanation of this phenomena).

The studies mentioned above investigated the behavior of a bubble or a group of bubbles in an infinite domain. However, in many practical applications, including novel biomedical applications (see Ref. 16 for references), bubbles are likely to be close to or attached to a wall or boundary. The presence of a wall would undoubtedly influence the oscillatory dynamics of the bubbles. Thus, there have been some studies investigating the influence of the wall on bubble oscillations (see review article by Blake and Gibson[19] and references therein) where the bubbles undergo a change in shape under large pressure fluctuations. For small pressure fluctuations, the main effect of the solid boundary is to change the natural frequencies of the collective bubble system. Recent experimental studies by Payne *et al.*[20] have mea-

[a)]Author to whom correspondence should be addressed. Electronic mail: a.ooi@unimelb.edu.au

sured the resonant frequency of identical bubbles attached to a rigid boundary. In the same study, Payne *et al.*[20] proposed to use an image-bubble concept, formulated as a coupled-oscillator problem, to model the behavior of a group of bubbles close to a wall. This approach was originally introduced by Strasberg[21] where he showed that a bubble oscillating close to a rigid boundary can be modeled by introducing a mirror-image bubble oscillating in phase with the original bubble. Thus, the net effect of the mirror-image bubble (and hence the wall) was to reduce the resonance frequency of the bubble. Payne *et al.*[20] showed that the mirror-image bubble approach can also be successfully extended to model the behavior of a group of bubbles close to a wall; predictions showed good agreement with the experimental data.

All the experimental studies conducted thus far have been for systems consisting of bubbles that are of the same size. For this type of system, it has been shown that the coupled-oscillator model predicts resonant frequencies that are in good agreement with experimental results. In the present work, an experimental and theoretical investigation was carried out to investigate the behavior of resonant frequencies for a system consisting of two or three different-sized bubbles on a rigid boundary. The theoretical model considered by Payne *et al.*[20] was extended to explain the experimental data of different-sized bubbles on a rigid boundary.

II. THEORETICAL DEVELOPMENT

It is commonly accepted that oscillations of large (millimeter sized) bubbles is governed by the following set of linear, second order ordinary differential equations

$$\ddot{\delta}_i(t) + \epsilon_i \dot{\delta}_i(t) + \omega_{oi}^2 \delta_i(t) = -\sum_{i \neq j}^{N} \frac{R_{oj}^2}{R_{oi} d_{ji}} \ddot{\delta}_j(t) \tag{1}$$

(see Ref. 22 and references therein) where $\delta_i(t) = R_i(t) - R_{oi}$, $R_i(t)$ is the radius of bubble i as a function of time, R_{oi} is the equilibrium radius of bubble i, and

$$\epsilon_i = \frac{4\mu}{\rho R_{0i}^2} \tag{2}$$

are the damping coefficients. Note that, in general, the damping is quite small and the mathematical expression for ϵ_i should include the radiation, thermal, and viscous damping. These expressions can get quite lengthy (see published works by Devin[23] and Eller[24]). In order to simplify the analysis, we follow the work of Ida[10] and use Eq. (2) as an approximation for the damping. The natural frequency of a bubble in isolation, ω_{oi}, is given by

$$\omega_{oi}^2 = \frac{3\gamma P_o}{\rho R_{oi}^2}, \tag{3}$$

where ρ is the density of the liquid, γ is the specific heat ratio, and P_o is the equilibrium pressure. Equation (1) can be written in matrix form as

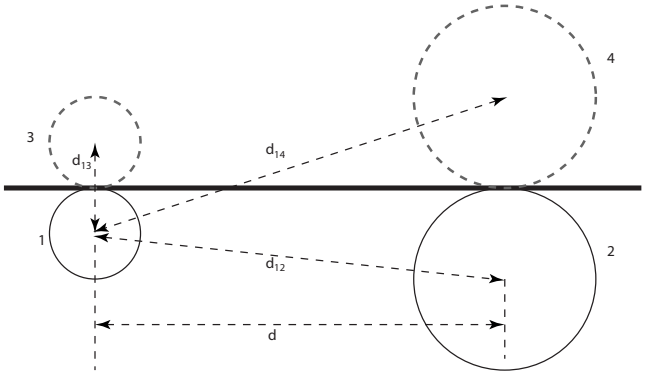

FIG. 1. Bubbles of different size close to a wall.

$$\mathbf{M}\ddot{\mathbf{x}} + \mathbf{C}\dot{\mathbf{x}} + \mathbf{K}\mathbf{x} = -\mathbf{S}\ddot{\mathbf{x}}, \tag{4}$$

where $\mathbf{x}$ is a time-dependent vector of all the $\delta_i(t)$, $\mathbf{M}$ is the inertia matrix, $\mathbf{C}$ is the damping matrix, $\mathbf{K}$ is the stiffness matrix, and $\mathbf{S}$ contains all the coupling terms of the bubble system. Equation (4) can be solved by assuming a solution of the form $\mathbf{x} = \mathbf{A}e^{\lambda t}$ which gives

$$[\lambda^2(\mathbf{M} + \mathbf{S}) + \lambda\mathbf{C} + \mathbf{K}]\mathbf{A} = 0. \tag{5}$$

In order to obtain a nontrivial solution for the right eigenvectors $\mathbf{A}$,

$$\det[\lambda^2(\mathbf{M} + \mathbf{S}) + \lambda\mathbf{C} + \mathbf{K}] = 0; \tag{6}$$

thus there are only distinct values of λ (eigenvalues) and associated $\mathbf{A}$ that can be solutions to Eq. (5). This is a quadratic eigenvalue problem and can be found to occur in many practical applications (see Ref. 25 for more examples). Equation (6) is a polynomial of order $2n$, where n is the matrix dimension or the number of bubbles in the system. Since all coefficients of the characteristic polynomial [Eq. (6)] are real numbers, the roots (eigenvalues) of Eq. (6) occur in n complex conjugate pairs. The natural frequencies of the system is given by the imaginary part of λ and the real part of λ (typically a negative constant) indicates the damping associated with the natural frequencies.

In general, closed form expressions for the eigenvalues and eigenvectors cannot be obtained. Numerical methods need to be employed to acquire the eigenvalues and eigenvectors and hence compute the solution to Eq. (4). However, insight into the solution can be obtained by examining the closed form expression for the eigenvalues of a simpler systems consisting of only two and three bubbles. First, consider the case where the system is made up of two bubbles with different equilibrium radii, R_{0i}, and the effects of the walls are modeled by the method of images (see Fig. 1). For such a system, Eq. (5) can be written explicitly as

$$\begin{bmatrix} 1 & 0 \\ 0 & 1 \end{bmatrix} \begin{bmatrix} \ddot{\delta}_1(t) \\ \ddot{\delta}_2(t) \end{bmatrix} + \begin{bmatrix} \epsilon_1 & 0 \\ 0 & \epsilon_2 \end{bmatrix} \begin{bmatrix} \dot{\delta}_1(t) \\ \dot{\delta}_2(t) \end{bmatrix} + \begin{bmatrix} \omega_{o1}^2 & 0 \\ 0 & \omega_{o2}^2 \end{bmatrix} \begin{bmatrix} \delta_1(t) \\ \delta_2(t) \end{bmatrix}$$
$$= - \begin{bmatrix} \dfrac{R_{o1}}{d_{13}} & \dfrac{R_{o2}^2}{R_{o1}d_{12}} + \dfrac{R_{o2}^2}{R_{o1}d_{14}} \\ \dfrac{R_{o1}^2}{R_{o2}d_{23}} + \dfrac{R_{o1}^2}{R_{o2}d_{21}} & \dfrac{R_{o2}}{d_{24}} \end{bmatrix} \begin{bmatrix} \ddot{\delta}_1(t) \\ \ddot{\delta}_2(t) \end{bmatrix}, \quad (7)$$

where d_{12} is the distance between the two real bubbles and the other d_{ij} are the distances between the bubbles and their images. Following the discussion above, a nontrivial solution can be only obtained if

$$\det \begin{bmatrix} \lambda^2\left(1 + \dfrac{R_{01}}{d_{13}}\right) + \lambda\epsilon_1 + \omega_{01}^2 & \lambda^2\left(\dfrac{R_{02}^2}{R_{01}d_{14}} + \dfrac{R_{02}^2}{R_{01}d_{12}}\right) \\ \lambda^2\left(\dfrac{R_{01}^2}{R_{02}d_{21}} + \dfrac{R_{01}^2}{R_{02}d_{23}}\right) & \lambda^2\left(1 + \dfrac{R_{02}}{d_{24}}\right) + \lambda\epsilon_2 + \omega_{02}^2 \end{bmatrix} = 0. \quad (8)$$

Equation (8) is the characteristic polynomial for a system of two unequally sized bubble with images used to model the effects of the wall.

The analytical expression for roots of the polynomial specified by Eq. (8) above can get unwieldy and does not provide useful information. A further simplification can be made if we assume that the two bubbles are of the same size, i.e., $R_{01}=R_{02}=R_0$ and thus $\omega_{01}=\omega_{02}=\omega_0$. We will also ignore damping by setting ϵ_i (for millimeter sized bubbles, the damping is usually very small) and assume that the size of the bubbles, R_0, is small relative to the distance between the bubbles, hence $d_{14}\approx d_{12}\approx d$ (see Fig. 1). Making these assumptions, Eq. (8) simplifies to

$$\det \begin{bmatrix} \lambda^2\left(\dfrac{3}{2}\right) + \omega_0^2 & \lambda^2\left(2\dfrac{R_0}{d}\right) \\ \lambda^2\left(2\dfrac{R_0}{d}\right) & \lambda^2\left(\dfrac{3}{2}\right) + \omega_0^2 \end{bmatrix} = 0. \quad (9)$$

The eigenvalues corresponding to Eq. (9), λ, can be found to be

$$\pm\sqrt{\frac{2\omega_0^2}{-3-4/(d/R_0)}} \quad \text{and} \quad \pm\sqrt{\frac{2\omega_0^2}{-3+4/(d/R_0)}}, \quad (10)$$

with associated eigenvectors given by

$$\begin{Bmatrix} 1 \\ 1 \end{Bmatrix} \quad \text{and} \quad \begin{Bmatrix} -1 \\ 1 \end{Bmatrix}. \quad (11)$$

The first eigenvector has a lower natural frequency and it represent a regime where the two bubbles oscillate in phase relative to each other. This is the + (symmetric) mode. The second eigenvector is the − (antisymmetric) mode because it represents the state where the two bubbles oscillate 180° out of phase with each other phase with each other. The + mode of a two bubble system always has a lower frequency than the − mode of a two bubble system. The reason for this was explained by Feuillade.[26] When bubbles oscillate in phase with each other, they expand and contract simultaneously. Because the liquid in between the bubbles is assumed to be incompressible, the motion of the bubbles is retarded and leads to a reduction in natural frequency. The opposite is true for the − mode leading to a higher natural frequency. Note that in the limit where $d\to\infty$, the natural frequencies of the system approach

$$\sqrt{\frac{2}{3}}\omega_0 \approx 0.8165\omega_0, \quad (12)$$

which is the natural frequency of a single bubble attached to a wall. A plot of the natural frequencies of the system is shown in Fig. 2 which is similar to Fig. 3 of Feuillade[8] who studied the oscillations of bubbles in free space. The only difference here is that the asymptotic value of the natural frequencies is approximately $0.8165\omega_0$ (as oppose to just ω_0) which is the result of adding image bubbles in the system to model effects of the wall.

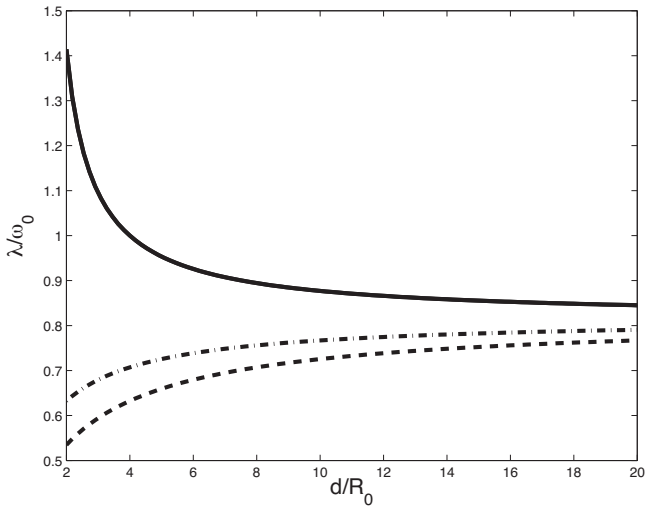

FIG. 2. Natural frequencies of the "−" mode for a two and three bubble system (—), natural frequencies for the "+" mode of a two bubble system (-·-), and natural frequency for the "+" mode of a three bubble system (---).

A similar analysis can be carried out for a system consisting of three bubbles arranged on the vertices of an equilateral triangle of length d attached to a wall. Again, the method of images will be used to model the effects of the wall and all bubbles will be assumed to be of equal size. The natural frequencies for such a system can be shown to be given by the following expressions:

$$\lambda = \pm\sqrt{\frac{2\omega_0^2}{-3-8/(d/R_0)}}, \quad \pm\sqrt{\frac{2\omega_0^2}{-3+4/(d/R_0)}}, \quad \pm\sqrt{\frac{2\omega_0^2}{-3+4/(d/R_0)}}.$$

Note that one of the eigenvalues is repeated. The corresponding eigenvectors are

$$\begin{Bmatrix} 1 \\ 1 \\ 1 \end{Bmatrix}, \quad \begin{Bmatrix} -1 \\ 1 \\ 0 \end{Bmatrix}, \quad \begin{Bmatrix} -1 \\ 0 \\ 1 \end{Bmatrix}. \quad (13)$$

The first eigenvector is the + (symmetric) mode because it represents the state where all three bubbles oscillate in phase. The other two eigenvectors have the same natural frequen-

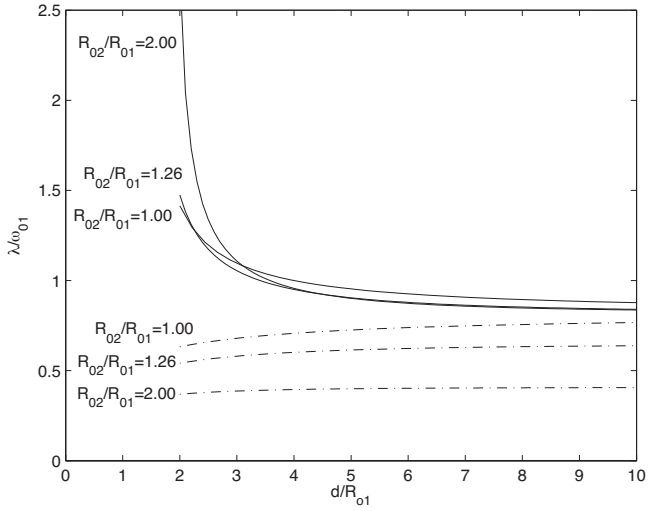

FIG. 3. Natural frequencies of a two bubble system close to a wall for different values of R_{02}/R_{01}. — Natural frequencies of the "−" mode, –·– Natural frequencies for the "+" mode.

cies and they represent a regime where two bubbles oscillate 180° out of phase with each other, while the third bubble remains in equilibrium (the − mode). Figure 2 also shows a plot of the natural frequencies of a three bubble system. The natural frequency associated with the − mode is the same as for the two bubble system. The frequency associated with the + mode is lower for the three bubble system than for the two bubble system.

The analysis above was formulated for bubbles that are of the same size. For a system consisting of bubbles that are of different sizes, the closed form solution can be unwieldy and not very informative. To study the effects of different bubble sizes, the eigenvalues for a two bubble system is obtained numerically by solving Eq. (8). Similar to the analysis carried out above, we will again assume that damping can be neglected and that the spacing between the bubbles are large compared to the size of the bubbles $d_{14} \approx d_{12}=d$. Computations were carried out with reference bubble size, $R_{01}=2.29$ mm and $R_{02}/R_{01}=1.00,1.29,2.00$. These bubble sizes were chosen because they are similar to the bubble size used in our experimental setup (see Sec. III). The resulting eigenvalues obtained are shown in Fig. 3 . The modes of oscillations can again be classified as either a symmetric (or +) mode where both bubbles oscillate in phase and antisymmetric (or −) mode where both bubbles oscillate 180° out of phase. As expected, and consistent with the reasons given by Feuillade[26] for the case with similar size bubbles, the frequency of the + mode is always less than the frequency of the − mode. From Fig. 3, it can be concluded that the − mode is affected by R_{02}/R_{01} only for small values of d/R_{01}. For $d/R_{01}>3$, there is very little variation in the natural frequency associated with the − mode. On the other hand, the + mode appears to be sensitive to the value of R_{02}/R_{01}. The natural frequency associated with the + mode appears to monotonically decrease with R_{02}/R_{01} for all values of d/R_{01}.

In the experiments, the bubble system was excited with an external source. So, strictly speaking, we will be measuring the resonance frequency of the bubble system. In systems where the damping is small, the resonance frequency is very similar to the natural frequency of the system. To investigate the behavior of system eigenmodal response to external excitation, we will take a closer look at the particular solution, $\boldsymbol{\delta}_p(t)$, of a two bubble system close to a wall [Eq. (7)] excited by a time harmonic force $\mathbf{q}(t)=\mathbf{q}_{\text{ext}}e^{i\omega_{\text{ext}}t}$. Following Tisseur and Meerbergen,[25] $\boldsymbol{\delta}_p(t)$ can be written as

$$\boldsymbol{\delta}_p(t) = e^{i\omega_{\text{ext}}t}\sum_{j=1}^{2n}\frac{\mathbf{B}_j^*\mathbf{q}_{\text{ext}}}{i\omega_{\text{ext}}-\lambda_j}\mathbf{A}_j \tag{14}$$

where $\mathbf{A}$, $\mathbf{B}$, and λ are right, left eigenvectors, and eigenvalues of the quadratic eigenvalue problem shown in Eq. (5). The contribution of the particular mode $\mathbf{A}_j$ to the particular solution is dependent on the jth coefficient

$$\phi_j = \left|\frac{\mathbf{B}_j^*\mathbf{q}_{\text{ext}}}{i\omega_{\text{ext}}-\lambda_j}\right|. \tag{15}$$

Thus ϕ is a measure of the contribution of the + or the − mode to the particular solution. It is clear that ϕ_j increases if we force the system at a frequency close to the eigenvalues associated with $\mathbf{A}_j$. A *resonance* condition in the system will occur if the frequency of the external excitation is very close to the natural frequencies (provided damping is small).

To study the effects of the external frequency excitation, the amplitude of the various modes, ϕ, is plotted as a function of excitation frequency. From Eq. (15) the peak of ϕ is expected to occur when the system is excited at the frequency similar to the natural frequency of the mode. If the same pressure amplitude were applied to both bubbles, then the response would only be made up by the + mode. However, if the pressure amplitudes applied to both both bubbles were different, then it could be expected that $\boldsymbol{\delta}_p(t)$ is made up of both the + and − modes. In the following graphs, results will be presented assuming that the external excitation is

$$\mathbf{q}_{\text{ext}} = W\begin{Bmatrix}1\\0.4\end{Bmatrix}. \tag{16}$$

These figures are selected because they are close to the amplitude of excitation that was applied to different bubbles in the experimental setup. In our experimental setup, all bubbles would experience different excitation amplitudes; hence $\boldsymbol{\delta}_p(t)$ will be made up of both the + and − modes. The magnitude of ϕ for both the + and − modes are shown Fig. 4. The effects of separation distance on ϕ is shown in Fig. 4(a). ϕ for the − mode is shown by the solid line and ϕ for the + mode is shown by the dashed line. As explained earlier, the peak of ϕ for the − mode will always occur at a frequency higher than the peak of ϕ for the + mode. It is clear that as the two bubbles are moved further apart, the − mode becomes the more dominant mode. The effects of bubble size ratio R_{02}/R_{01} on the amplitudes of the different modes is illustrated in Fig. 4(b). It is clear that increasing the size of the second bubble increases the amplitude of the + mode while preserving the peak corresponding to the − mode. Hence one can reasonably expect the + mode to be more dominant for larger values of R_{02}/R_{01}.

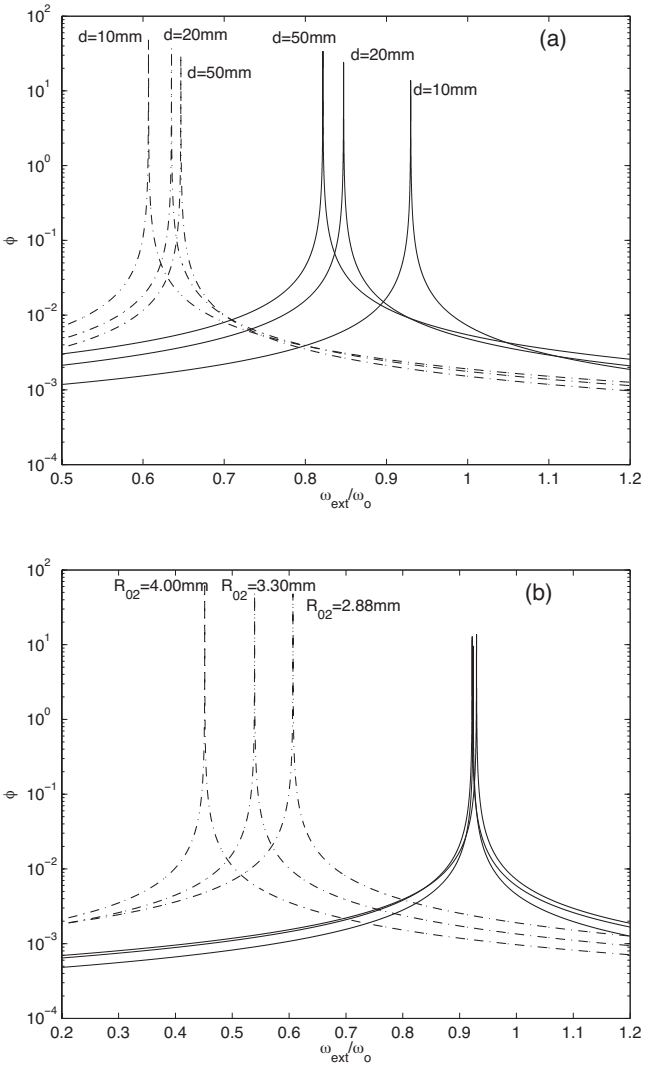

FIG. 4. Amplitude of "+" mode (–·–) and amplitude of "−" mode (—) as a function of excitation frequency ω_{ext}. (a) illustrates the effects of varying distance between the bubbles, d, which is indicated in the figure. R_{01} =2.29 mm and R_{02}=2.88 mm. The effects of varying R_{02} is shown in (b), where d=10 mm and R_{01}=2.29 mm. The values of R_{02} is shown in the figure.

III. EXPERIMENTAL SETUP

The principal purpose of the experimental apparatus is to transfer acoustic energy to the bubble system and to detect the system's response. The apparatus utilized is shown in Fig. 5. The rig and postprocessing methodology is very similar to that used by Payne *et al.*[20] The excitation signal is generated by a computer and is passed into a stereo amplifier. The amplified signal is then passed into the mechanical oscillatory unit which converts the electrical signal into oscillations in the liquid where the bubbles exist. The response of the bubble system is detected by a hydrophone and this signal is amplified by a charge amplifier unit. The bubble oscillations are logged using a high speed data acquisition system consisting of a data card, a data adapter, and a data logging computer.

The chamber is made from 12 mm thick acrylic and has a square base of length of 300 mm and height of 50 mm. A 30 mm diameter circular hole in the bottom of the cylinder

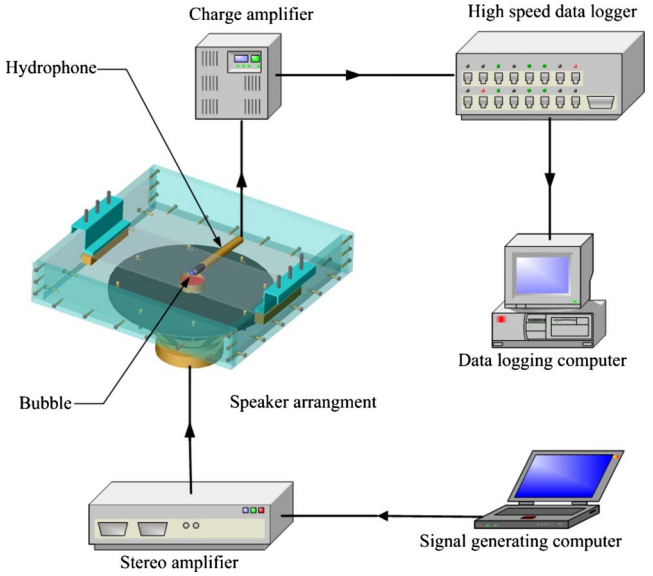

FIG. 5. (Color online) Experimental apparatus.

allows the acoustic waves to propagate through the liquid domain. To generate the mechanical oscillations, a common audio speaker was adopted which is similar to that used by Hsiao.[9] It was a 203.2 mm diameter, 8 Ω speaker and was modified by the attachment of an aluminum piston to its diaphragm. The piston in turn drove a piece of duct tape that sealed the hole in the chamber base.

The water in the tank was Melbourne tap water which had been filtered prior to filling the tank. The bubbles were introduced manually with a precision syringe (50 μl, Alltech Associates Australia, with a volumetric accuracy of ±5%) fitted with a needle, and were arranged as close as possible to the centerline of the piston as possible (±0.25 mm). The error in injected bubble volume corresponded to less than 1.7% of the bubble radii. Prior to this any small bubbles that have been introduced by the process of filling the tank were carefully removed by a combination of sweeping the plate surface with a wire and suction using a syringe and tube. Introduction of all the bubbles required generally took a few minutes and where bubble sizes were varied; this was done by injection of additional air. When a bubble was moved to a new location, it was swept with a wire. It is well-known that very small bubbles can increase their size over time, owing to rectified diffusion:[27] even under very low-amplitude forcing, bubbles with radii in the order of 100 μm can increase their radius by 50% after 1 h of continuous forcing.[28] However, since the bubbles of the present experiment were millimeter-sized bubbles (4000 times the volume of the just-cited experiments) and forcing pressures were less than 10^{-6} bar, for rectified diffusion or dissolution effects were negligible over the approximately 45–60 min required to perform a complete set of measurements. Careful observation indicated the bubble size had not changed measurably (to ±0.1 mm) before and after the experiments. Sound amplitudes were kept well below those at which bubbles moved or exhibited surface oscillations.

A chirp signal was used to drive the speaker; it had constant amplitude and increased in frequency over time.

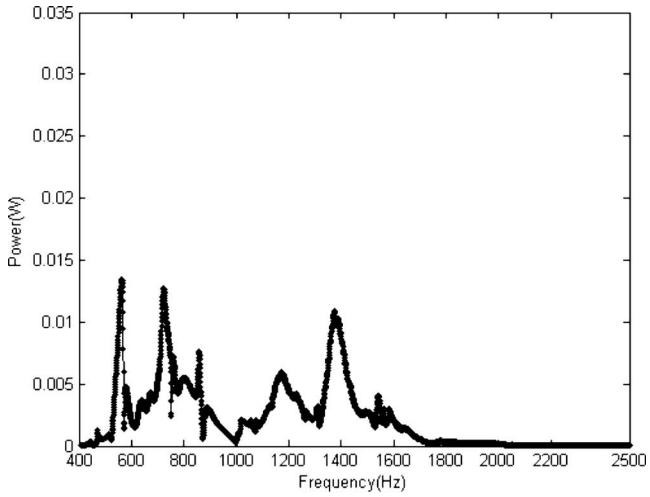

(a)

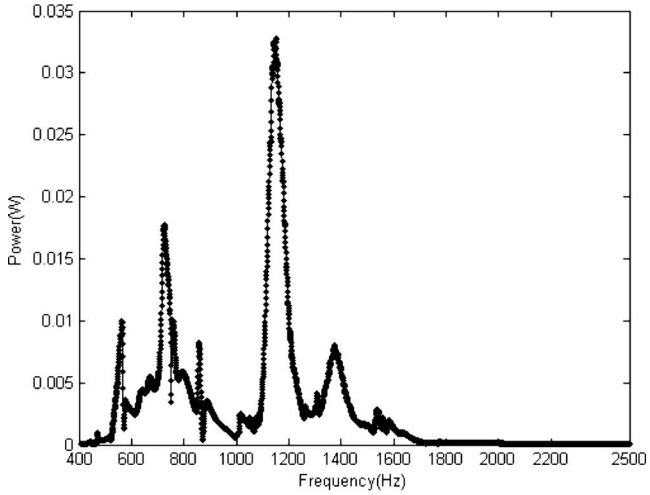

(b)

FIG. 6. Frequency domain response for an input chirp signal. (a) Without bubble response. (b) Response for a 50 μl bubble.

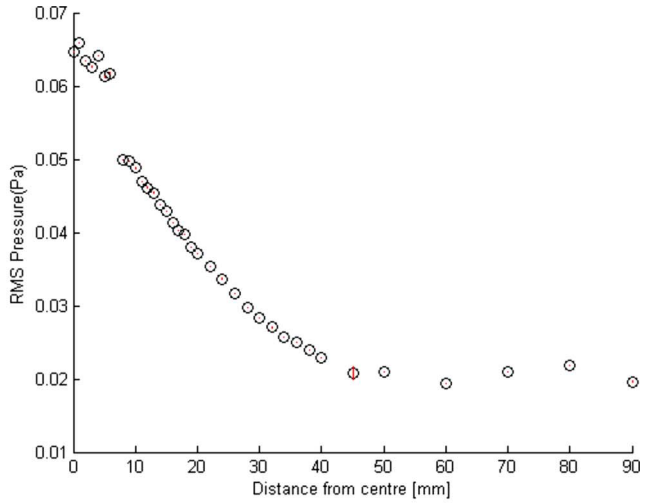

(a) Pressure distribution in the y direction

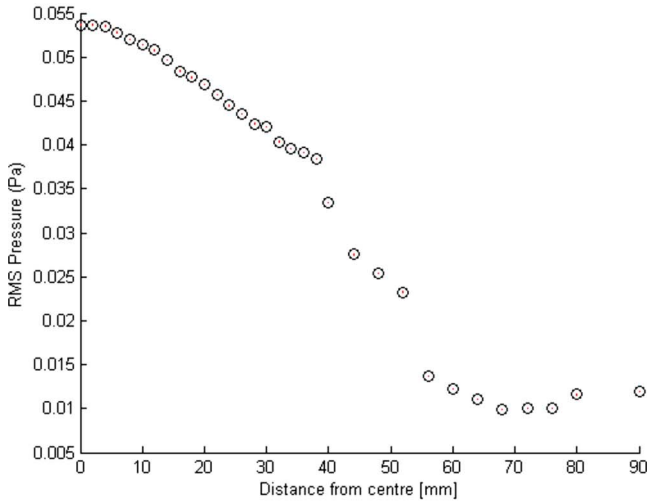

(b) Pressure distribution in the x direction

FIG. 7. (Color online) Pressure distribution in the x-y direction of the tank.

This signal was amplified before it was passed through to the speaker. The length of the chirp signal was kept constant at 480 ms; its frequency varied from 100 to 2500 Hz, covering the expected resonance of the bubble system in the tank. Chirps were run in rapid succession, 540 ms apart.

Thirty time domain chirp responses were detected via the hydrophone and were converted to the frequency domain via a fast Fourier transform. As a reference, and in order to determine the frequency response of the tank itself, data from the hydrophone were initially obtained for cases when no bubbles were present in the tank.[20] Typical frequency response is shown in Fig. 6(a). Experiments were subsequently carried out with bubble systems present in the tank. Typical frequency response when there is a single 50 μl bubble present in the tank is shown in Fig. 6(b). In order to obtain the resonance frequency of the bubble system, the data in Fig. 6(b) were scaled with the data in Fig. 6(a) and the resonance frequency of the bubble system is identified as the frequency when the scaled value is a maximum.

Experiments were conducted to detect pressure variations along the plate surface. The hydrophone was placed at the center of the acoustic source and directed away from the source in two directions normal to each other along the plate. As the pressure oscillations are cyclic, the rms value of the pressure is calculated for a given chirp length of 0.18 ms, with frequency varying from 800–1500 Hz. The rms pressure is calculated using the Euclidean length of the set of pressures given as

$$\|P_{ch}\| = \sqrt{\sum_{i=1}^{N_{cl}} P_{ch}(i)^2}, \tag{17}$$

where the $P_{ch}(i)$ is an element of the set of pressures which changes with time and N_{cl} is the length of the set of pressures. This Euclidean length is then converted to a rms value by considering

$$P_{\text{rms}} = \frac{\|P_{ch}\|}{\sqrt{N_{cl}}}. \tag{18}$$

This rms pressure value represented as a voltage value is shown in Fig. 7 for two orthogonal directions, considered in

the experiment. The hydrophone was placed as close to the plate as physically possible to detect the pressure oscillations at the plate.

Figure 7(a) depicts the pressure distribution along the axis denoted as x; the figure shows that pressure is highest where the hydrophone is directly above the acoustic source. As the distance from the acoustic source increases, the pressure decreases accordingly. The wavelengths of sound in the tank were at least 1 m, and the distance from the source to the tank wall was 0.15 m. The disk creating the oscillation in the tank was only 15 mm in radius, and therefore might be considered a point source relative to the wavelength. The sound field intensity falls off to 0.2 of its maximum value over only 5% of a wavelength, not because of standing-wave effects but simply because of the geometric spreading of the sound wave from the small source. Figure 7(b) depicts the pressure distribution along the axis denoted as y. Figures 7(b) and 7(a) are similar, yet differences between the plots exist. Note that the variations in the pressure was calculated for ten signals and the standard deviation is plotted which is barely visible. It could be considered that random errors due to signal generation and detection are insignificant.

In Secs. IV and V, when experimental data are compared with theoretical predictions, we will assume that the resonance frequency is similar to the natural frequency [obtained by solving Eq. (6)]. In the bubble system analyzed in this paper, the damping is usually very small. In general, it is well-known that the resonance frequency is very close to the natural frequency for a linear second order system with small damping. Justification of this assumption for a bubble system close to a wall can be found in Ref. 20.

IV. RESULTS AND DISCUSSION

As mentioned previously, this study will focus on the comparison of image-bubble theory with experimental data for a system consisting of bubbles of different sizes. As far as the authors are aware, this type of data has not been acquired before. Studies in the literature on equally sized bubbles (see Refs. 8, 10, 29, and 20) show that the coupled-oscillator model using image theory predicts resonant frequencies that agree well with experimental data. Practical applications usually consist of systems with bubbles that are of different sizes. Thus, it is important to investigate and prove if this agreement extends to data from a system made up of bubbles that are of different sizes. In order to keep the number of parameters manageable, only two and three bubble arrangements will be considered. For the three bubble system, the bubbles are arranged on the vertices of an equilateral triangle.

Experiments were conducted for two different-sized bubbles where the bubbles were positioned next to each other with a separation distance of 12 mm. One 50 μl bubble was left as the reference bubble next to a second bubble which varied in size. The hydrophone was placed at the center of the two bubbles to detect the oscillations of the two bubble system. The size of the second bubble was incrementally increased from 5 to 400 μl. At each increment the resonance frequency of the bubble system was measured. The

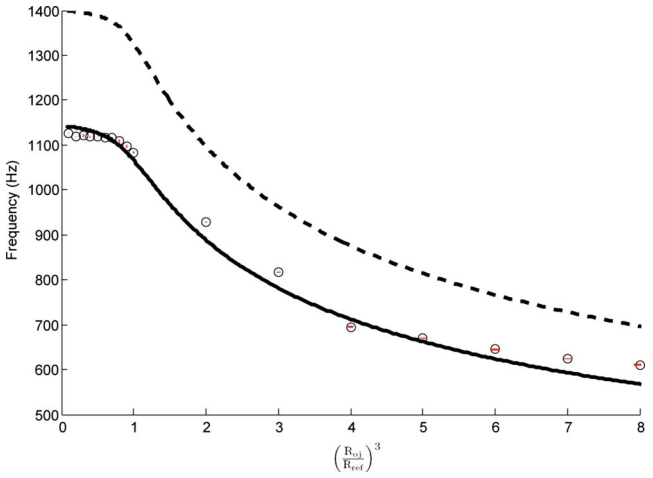

FIG. 8. (Color online) Resonance frequency vs ratio of bubble radius for two different-sized bubbles where the reference bubble remains at 50 μl ($R_{01}=R_{\mathrm{ref}}=2.29$ mm) and the other bubble incrementally increased size from 5 to 400 μl. (---) Symmetric mode eigenvalues from Eq. (5) without image bubbles, (—) with image bubbles. (○) The experimental results, with error bars shown by vertical lines.

results obtained for this two bubble system are shown in Fig. 8. The error bars on the figure are smaller than the symbols, showing that there was insignificant variation between the 30 chirps. The wavelength of acoustic pressure waves in the chamber was large relative to the distance between the bubbles. Hence, it could be assumed that the chirp signal excited the symmetric mode (where all bubbles oscillate in phase) of the system and the dominant frequency detected by the hydrophone would be the + mode frequency, especially if the bubbles were close. The theoretical + mode frequency using image bubbles to approximate the effects of the wall [i.e., the roots of Eq. (8)] is plotted against the ratio of the bubble sizes, namely, the ratio between the size of the volume incremented bubble and the reference bubble [i.e., $(R_{oj}/R_{\mathrm{ref}})^3$]. Note that for these set of results, $R_{\mathrm{ref}}=R_{01}=2.29$ mm. For comparison, the symmetric mode natural frequency for a bubble system in an unbounded domain (i.e., without image bubbles) is also shown in this figure. It is clear that the experimental data lie closer to the eigenvalues given by Eq. (8), validating the use of image bubbles to model wall effects.

Figure 8 shows that for small values of $(R_{oj}/R_{\mathrm{ref}})^3 \ll 1$, the system response is dominated by the larger 50 μl bubble on a wall. Using Eqs. (3) and (12) the + mode natural frequency of a 50 μl bubble on the wall is approximately 1163 Hz. This is very close to the resonance frequency measured by the hydrophone when $(R_{oj}/R_{\mathrm{ref}})^3 \ll 1$. As $(R_{oj}/R_{\mathrm{ref}})^3$ increases, the resonance requency decreases, consistent with the theoretical prediction shown in Fig. 3. When $(R_{oj}/R_{\mathrm{ref}})^3 > 6$, the experimental resonant frequency is larger than the theoretical prediction made using the mirror image. The bigger (dominant) bubble in the system is no longer the reference 50 μl but the other bubble in the system, which could be up to 400 μl in volume. This deviation from the experimental data could be partially explained using the argument presented by Strasberg.[21] When bubbles get bigger, buoyancy and surface tension forces change the shape of the

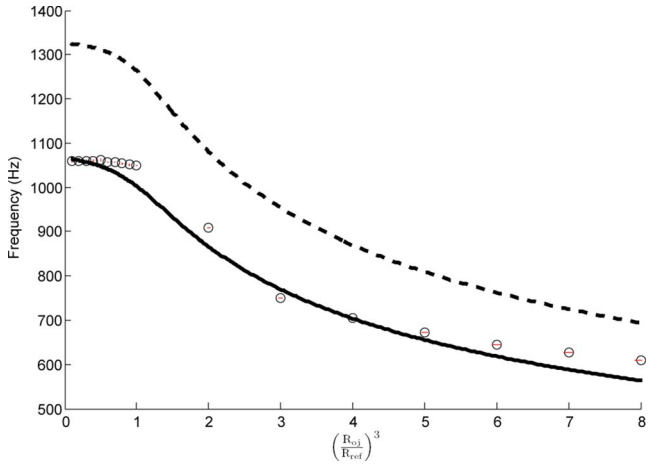

FIG. 9. (Color online) Resonance frequency vs ratio of bubble radius for three different-sized bubbles with two reference bubbles remains at 50 μl ($R_{01}=R_{\mathrm{ref}}=2.29$ mm) and the other bubbles incrementally increases from 5 to 400 μl for each experi ments. (---) Symmetric mode eigenvalues from Eq. (5) without image bubbles and (—) with image bubbles. (○) The experimental results, with error bars shown by vertical lines.

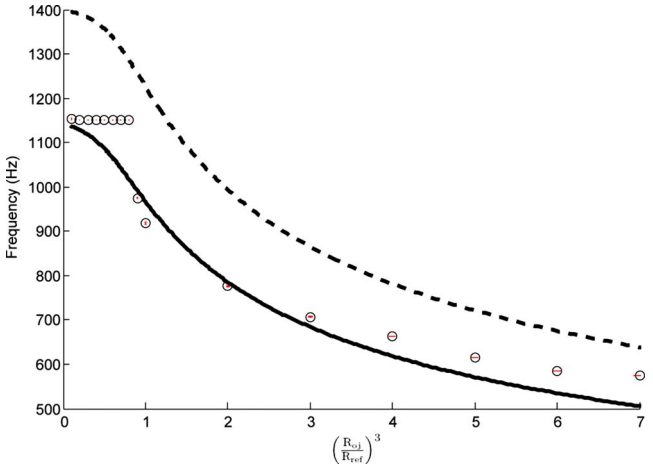

FIG. 10. (Color online) Resonance frequency vs ratio of bubble radius for three different-sized bubbles with one reference bubble at 50 μl ($R_{01}=R_{\mathrm{ref}}=2.29$ mm) and the other two bubbles incrementally increase size from 5 to 350 μl with each experiment. (---) Eigenvalues from Eq. (5) without image bubbles and (—) with image bubbles. (○) The experimental results, with error bars shown by vertical lines.

bubbles from a perfect sphere to an oblate spheroid. The theoretical analysis carried out by Strasberg[21] showed that this change in shape can cause a slight increase in the resonance frequency of bubbles in an unbounded domain. Even though the bubbles here are close to a wall, we argue that similar principles would apply. This slight increase in the measured frequency is also consistent with the results presented in Ref. 20.

Similar to the two different-sized bubble case, experiments were conducted for a system with three different-sized bubbles. Two different cases are possible. The first case is where a single bubble is incrementally increased in volume with each experiment, leaving two other bubbles as reference bubbles. In our experiments, the volume of the (two) reference bubbles were fixed at 50 μl, and the volume of the incrementally growing bubble was varied from 5 to 400 μl. The resonance frequencies measured by the experimental apparatus is shown in Fig. 9. The second case is where two bubbles incrementally increase in volume, leaving one bubble as the reference bubble. In our experiments, the volume of the reference bubble was kept constant at 50 μl and the size of the other two bubbles were varied from 5 to 350 μl. The results obtained are shown in Fig. 10. In both these cases the bubble separation distance was kept constant. Preliminary tests had showed that the positioning of the hydrophone had little effect on the measured + mode resonance frequency. Hence the hydrophone was placed close to the reference bubble, to be consistent with all the other experiments presented in this paper.

There are general similarities between data in Figs. 9 and 10. It is clear that there is a decrease in the symmetric mode resonance frequency for increasing values of $(R_{oj}/R_{\mathrm{ref}})^3$. The prediction using the mirror-image theory is plotted in these figures and, for reference, the + mode natural frequency of three bubbles in an unbounded domain (i.e., no image bubbles) is also shown in Figs. 9 and 10. Similar to the previous two bubble case, it is clear that the image theory provides a better match with the experimental data. In Fig. 9 and for $(R_{oj}/R_{\mathrm{ref}})^3 \ll 1$, the bigger (dominant) bubble in the system are the two reference 50 μl bubbles. It can reasonably be expected that the two 50 μl bubbles will dominate the response of the system for $(R_{oj}/R_{\mathrm{ref}})^3 \ll 1$. Thus one can simply ignore the third smaller bubble in the system and predict the resonance frequency by using Eq. (10). This gives the natural frequency of two 50 μl bubbles on a wall to be 1038 Hz, which is very close to the frequency measured experimentally for $(R_{oj}/R_{\mathrm{ref}})^3 \ll 1$ (see Fig. 9). When there is only one reference bubble in the three bubble system, the bigger (dominant) bubble in the system is the reference 50 μl when $(R_{oj}/R_{\mathrm{ref}})^3 \ll 1$. Figure 10 shows that for $(R_{oj}/R_{\mathrm{ref}})^3 \ll 1$, the measured frequency is approximately 1150 Hz. This is very close to the value of the natural frequency for a single 50 μl bubble attached to a wall which has a natural frequency of 1163 Hz. Hence, the effects of the two neighboring bubbles can be neglected provided that $(R_{oj}/R_{\mathrm{ref}})^3 \ll 1$.

There are, however, several differences worth mentioning when comparing data in Figs. 9 and 10. For $(R_{oj}/R_{\mathrm{ref}})^3 > 3$, it is clear that there is better agreement with theoretical predictions in Fig. 9 than in Fig. 10. In Fig. 10, there are two large bubbles in the system that are shaped like oblate spheroids. Since Strasberg[21] showed that the natural frequency of the system is increased for bubbles shaped like oblate spheroids, and since the measured frequencies are dominated by the larger bubbles in the system, the two larger bubbles shift the resonance frequency above the curve predicted by the mirror-image theory. In Fig. 9 with $(R_{oj}/R_{\mathrm{ref}})^3 > 3$, only one of the bubbles in the system was large (and shaped like an oblate spheroid); thus there is better agreement with predicted data. This shows that as the number of large bubbles increase, deviation from the theory developed here is more prominent. This is to be expected because the theory assumes that the bubbles are spherical, which is not the case when the bubbles are large.

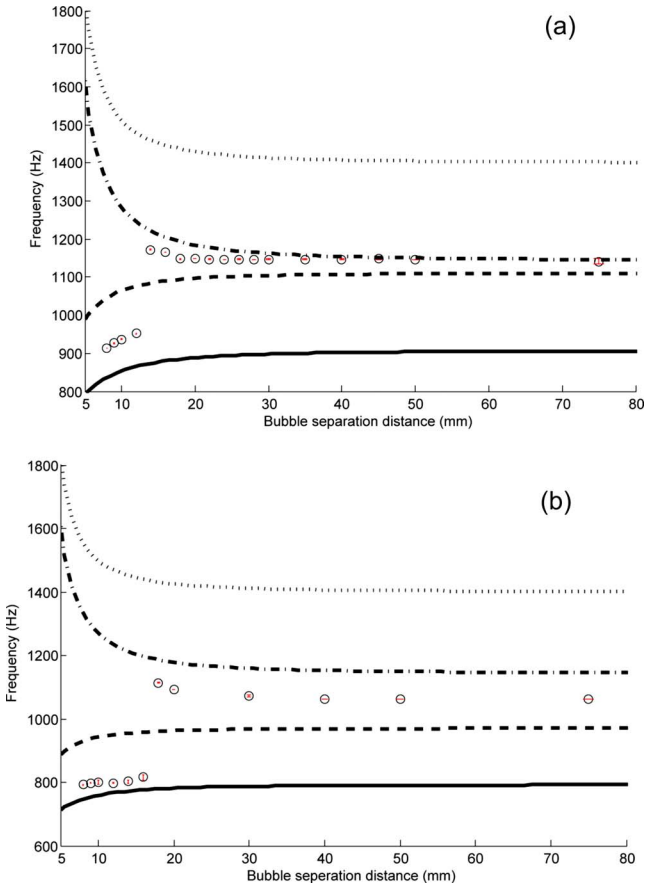

FIG. 11. (Color online) Resonance frequency vs bubble separation distance for two bubbles of 50 μl ($R_{01}=R_{\text{ref}}=2.29$ mm) and 100 μl ($R_{02}=2.88$ mm) (a) 150 μl ($R_{02}=3.30$ mm) (b). (---) symmetric and (···) antisymmetric mode eigenvalues for the mathematical model without any image bubbles. (—) symmetric and (–·–) antisymmetric mode eigenvalues using image bubbles to model the effects of the wall. (○) Experimental data, with error bars shown by vertical lines.

In the next set of experiments, the effect of bubble separation on the resonant frequency for a system of two different-sized bubbles is investigated. Experiments were conducted with two different-sized bubbles. The bubbles were initially placed close to each other and then one of the bubbles were gradually moved further away from the reference bubble. The first set of experiments were conducted with a 50 μl bubble placed next to a 100 μl ($r=R_{02}/R_{01}\approx 1.26$) bubble with a separation distance of 8 mm. The bubbles were then moved along the rigid boundary until the bubble separation distance reached 80 mm. The results obtained are shown in Fig. 11(a). To illustrate the effects of the wall, theoretical predictions were computed for cases with (to simulate wall effects) and without image bubbles in the model. In general, it is clear that the predicted data obtained using image bubbles tend to agree better with the experimental data. For small bubble separation, the dominant frequency is the + mode frequency. As the bubbles are moved further apart, the frequency response is dominated by the − mode. It can be seen that the + mode frequency predicted by the theoretical results deviate considerably from the experimental data. But as the distance between the bubbles increase, it seems that the − mode begins to dominate and there is better agreement with theoretical predictions. The occurrence of the

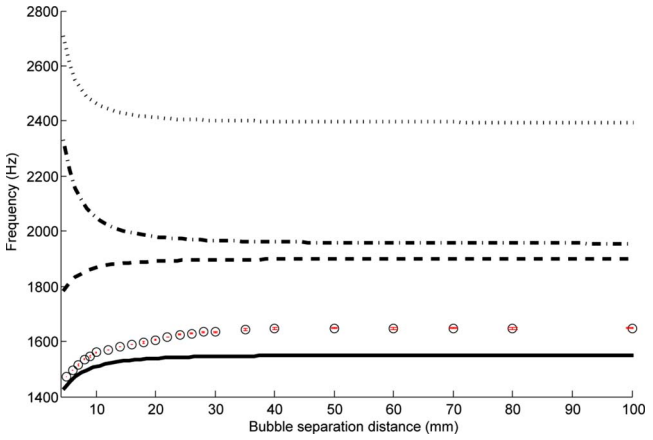

FIG. 12. (Color online) Resonance frequency vs bubble separation distance for two bubbles of 10 μl ($R_{01}=R_{\text{ref}}=1.34$ mm) and 20 μl ($R_{02}=1.68$ mm). (---) Symmetric and (···) antisymmetric mode eigenvalues for the mathematical model without any image bubbles. (—) Symmetric and (–·–) antisymmetric mode eigenvalues using image bubbles to model the effects of the wall. (○) Experimental data, with error bars shown by vertical lines.

− mode is likely to be due to the fact that the applied sound field was not perfectly uniform within the chamber. As shown previously in Fig. 7, the pressure is high at the center of the piston and decreases away from the piston center. As shown in Fig. 11(a), the theoretically predicted − mode shows closer agreement to the experimental data. The changeover from + to − mode occurs as the distance between the bubbles reaches approximately 14 mm, and the − mode appears to continue to dominate for bubble separation distances beyond 14 mm.

From the theoretical analysis described in Sec. II, it was conjectured that the − mode would be more difficult to excite at larger values of r. In order to prove this hypothesis, an experiment was conducted for a two bubble system with a larger value of r. This was achieved by keeping the reference bubble at 50 μl and increasing the size of the second bubble to 150 μl. This system would correspond to $r\approx 1.44$. Again, as in the previous case, the bubbles were moved apart to a maximum distance of 80 mm. The results obtained are shown in the Fig. 11(b). As in the previous case, for small values of d, the dominant frequency is the + mode frequency. The − mode becomes dominant when the distance between the bubble was increased. It is important to note that the transition of the dominant frequency from the + to the − mode occurs at bubble separation $d\approx 20$ mm. This is a larger transition value than for the prior set of experiment (when the transition occurs at $d\approx 14$ mm), indicating that the antisymmetric mode is harder to excite in this system (i.e., for $r\approx 1.44$) than in the previous system (for $r\approx 1.26$).

Lastly, the effects of smaller bubble size is investigated. Experiments were conducted with a bubble system consisting of 10 μl and a 20 μl bubbles. This case has $r\approx 1.26$ [similar to the case in Fig. 11(a)] but d/R_0 is much larger (due to the smaller size of the 10 μl reference bubble). The results obtained are shown in Fig. 12. It is clear that the dominant frequency obtained is the + mode resonance frequency. No − mode frequencies were detected by the microphone. The + mode resonance is closer to that of the theoretically predicted when the distance between the bubbles is

small. However, as the bubble separation distance increases, the experimental data deviate from the theoretical values. The + mode frequency increases gradually and asymptotes, similar to that predicted by the mathematical model. However, the experimental results and the theoretical results do not asymptote to the same value. It is interesting to note that for all separation distances, the experimentally measured resonance frequency did not pick up the − mode frequency.

V. CONCLUSION

The present results on bubble attached to a rigid boundary show that bubbles of different sizes exhibit similar trends in resonant acoustic frequency to bubbles of equal size. It has been illustrated that as in the case of systems consisting of bubbles that are of the similar size, the oscillations of a system of bubbles of different size attached to a rigid boundary can be modeled using coupled-oscillator theory with mirror-image bubbles approximating the effects of the wall. Both theory and experimental data show that as the ratio of the volume of the bubbles in the system increases, the resonance frequency of the system decreases. Results obtained using the coupled-oscillator model were generally in fair to good agreement with the experimental data. It was observed that when the distance between the bubbles is small, the symmetric mode is dominant and when the distance between the bubbles is large, the antisymmetric mode frequency becomes dominant. The antisymmetric mode is harder to detect when the ratio of the bubble sizes in the system is large.

[1]L. Rayleigh, "On the pressure developed in a liquid during the collapse of a spherical cavity," Philos. Mag. **34**, 94–98 (1917).
[2]M. S. Plesset, "The dynamics of cavitation bubbles," J. Appl. Mech. **2**, 277–282 (1949).
[3]E. A. Neppiras and B. E. Noltingk, "Cavitation produced by ultrasonics," Proc. Phys. Soc. London, Sect. B **63**, 674–685 (1950).
[4]M. Poritsky, "The collapse on growth of a spherical bubble on cavity in a viscous fluid," Proceedings of the First U.S. National Congress on Applied Mechanics, Illinoise Institute of Technology, June 11–16, 813–821 (1952).
[5]M. Minnaert, "On musical air bubbles and the sound of running water," Philos. Mag. **16**, 235–248 (1933).
[6]A. Ooi, A. Nikolovska, and R. Manasseh, "Analysis of time delay effects on a linear bubble chain system," J. Acoust. Soc. Am. **124**, 815–826 (2008).
[7]I. Tolstoy, "Superresonant systems of scatterers. I," J. Acoust. Soc. Am. **80**, 282–294 (1986).
[8]C. Feuillade and M. F. Werby, "Resonances of deformed gas bubbles in liquids," J. Acoust. Soc. Am. **96**, 3684–3692 (1994).
[9]P. Y. Hsiao, M. Devaud, and J. Bacri, "Acoustic coupling between two air bubbles in water," Eur. Phys. J. E **4**, 5–10 (2001).
[10]M. Ida, "A characteristic frequency of two mutually interacting gas bubbles in an acoustic field," Phys. Lett. A **297**, 210–217 (2002).
[11]R. Manasseh, A. Nikolovska, A. Ooi, and S. Yoshida, "Anisotropy in the sound field generated by a bubble chain," J. Sound Vib. **278**, 807–823 (2004).
[12]A. A. Doinikov, R. Manasseh, and A. Ooi, "On time delays in coupled multibubble systems," J. Acoust. Soc. Am. **117**, 47–50 (2005).
[13]V. Leroy, M. Devaud, T. Hocquet, and J.-C. Bacri, "The bubble cloud as an n-degree of freedom harmonic oscillator," Eur. Phys. J. E **17**, 189–198 (2005).
[14]A. Nikolovska, R. Manasseh, and A. Ooi, "On the propagation of acoustic energy in the vicinity of a bubble chain," J. Sound Vib. **306**, 507–523 (2007).
[15]V. Leroy, A. Strybulevych, M. Scanlon, and J. Page, "Transmission of ultrasound through a single layer of bubbles," Eur. Phys. J. E **29**, 123–130 (2009).
[16]R. Manasseh and A. Ooi, "The frequencies of acoustically interacting bubbles," Bubble Science, Engineering and Technology **82**, 58–74 (2009).
[17]R. Mettin, I. Akhatov, U. Parlitz, C.-D. Ohl, and W. Lauterborn, "Bjerknes forces between small cavitation bubbles in a strong acoustic field," Phys. Rev. E **56**, 2924–2931 (1997).
[18]C. Feuillade, "Acoustically coupled gas bubbles in fluids: Time-domain phenomena," J. Acoust. Soc. Am. **109**, 2606–2615 (2001).
[19]J. R. Blake and D. C. Gibson, "Cavitation bubbles near boundaries," Annu. Rev. Fluid Mech. **19**, 99–123 (1987).
[20]E. M. B. Payne, S. J. Illesinghe, A. Ooi, and R. Manasseh, "Symmetric mode resonance of bubbles attached to a rigid boundary," J. Acoust. Soc. Am. **118**, 2841–2849 (2005).
[21]M. Strasberg, "The pulsation frequency of nonspherical gas bubbles in liquids," J. Acoust. Soc. Am. **25**, 536–537 (1953).
[22]M. Ida, "Avoided crossings in three coupled oscillators as a model system of acoustic bubbles," Phys. Rev. E **72**, 036306 (2005).
[23]C. J. Devin, "Survey of thermal radiation, and viscous damping of pulsating air bubbles in water," J. Acoust. Soc. Am. **31**, 1654–1667 (1959).
[24]A. I. Eller, "Damping constants of pulsating bubbles," J. Acoust. Soc. Am. **47**, 1469–1470 (1959).
[25]F. Tisseur and K. Meerbergen, "The quadratic eigenvalue problem," SIAM Rev. **43**, 235–286 (2001).
[26]C. Feuillade, "Scattering from collective modes of air bubbles in water and the physical mechanism of superresonances," J. Acoust. Soc. Am. **98**, 1178–1190 (1995).
[27]T. G. Leighton, *The Acoustic Bubble* (Academic, London, 1994).
[28]P. Tho, R. Manasseh, and A. Ooi, "Cavitation microstreaming patterns in single and multiple bubble systems," J. Fluid Mech. **576**, 191–233 (2007).
[29]M. Ida, "Alternative interpretation of the sign reversal of secondary Bjerknes force acting between two pulsating gas bubbles," Phys. Rev. E **67**, 056617 (2003).